

Effect of the Diisocyanate Structure and the Molecular Weight of Diols on Bio-Based Polyurethanes

Wannarat Panwiriyarat,^{1,2} Varaporn Tanrattanakul,¹ Jean-François Pilard,² Pamela Pasetto,² Chuanpit Khaokong¹

¹Department of Materials Science and Technology, Bioplastic Research Unit, Faculty of Science, Prince of Songkla University, Songkhla 90112, Thailand

²Institut des Molécules et Matériaux du Mans, UMR CNRS 6283, Université du Maine, 72085, Le Mans Cedex, France

Correspondence to: V. Tanrattanakul (E-mail: varaporn.t@psu.ac.th)

ABSTRACT: Bio-based polyurethanes (PU) containing poly(ϵ -caprolactone) diol (PCL) and hydroxyl telechelic natural rubber (HTNR) were synthesized. The effect of the diisocyanate structure and the molecular weights of diols on the mechanical properties of PU were investigated. Three different molecular structures of diisocyanate were employed: an aliphatic diisocyanate (hexamethylene diisocyanate, HDI), an aromatic diisocyanate (toluene-2,4-diisocyanate, TDI) and a cycloalkane diisocyanate (isophorone diisocyanate, IPDI). Two molecular weights of each diol were selected. When HDI was employed, a crystalline PU was generated while asymmetrical structures of TDI and IPDI provided an amorphous PU. The presence of crystalline domains was responsible of a change in tensile behavior and physical properties. PU containing TDI and IPDI showed a rubber-like behavior: low Young's modulus and high elongation at break. The crystalline domains in PU containing HDI acted as physical crosslinks, enhancing the Young's modulus and reducing the elongation at break, and they are responsible of the plastic yielding. The crystallinity increased the tear strength, the hardness and the thermal stability of PU. There was no significant difference between the TDI and IPDI on the mechanical properties and the physical characteristics. Higher molecular weight of PCL diol changed tensile behavior from the rubber-like materials to the plastic yielding. Thermal and dynamic mechanical properties were determined by using DSC, TGA and DMTA. © 2013 Wiley Periodicals, Inc. *J. Appl. Polym. Sci.* 130: 453–462, 2013

KEYWORDS: biodegradable; biopolymers and renewable polymers; polyurethanes; copolymers; elastomers

Received 9 August 2012; accepted 16 January 2013; published online 19 March 2013

DOI: 10.1002/app.39170

INTRODUCTION

Polyurethane is generally prepared via a polyaddition reaction between a diisocyanate and a polyol to form urethane linkages. Its molecular structure and its properties vary over a broad range of stiffness or flexibility, hardness, and density,¹ consequently there are many applications of polyurethane such as flexible or rigid foams, chemical resistant coatings, rigid and flexible plastics, specialty adhesives and sealants, and elastomers,² all of which lead to an increase in polyurethane consumption. At the end of their life cycle, these synthetic polymers so widely used do not degrade naturally leading to a considerable amount of waste and, as consequence, to environmental issues. In this context, the development of biodegradable polyurethane is a topic of interest. Among the commercial biodegradable polymers, such as polyhydroxyalkanoates, poly(lactic acid), and polyesteramide, poly(ϵ -caprolactone) (PCL) diol has been widely used as a starting material for synthesizing biode-

gradable polyurethane, which can now be found in many applications.^{3–18}

The synthesis of bio-based polyurethanes in general has gained interest as well. To find alternative renewable monomer feedstocks and to promote sustainable development, many bio-based polyols from renewable resources, such as plant oil,^{19–23} sugar,²⁴ chitosan,²⁵ natural rubber,^{26–39} chitin,^{40,41} glucan,⁴² and heparin⁴³ have been explored for polyurethane synthesis. Natural rubber can be easily chemically modified to give a functionalized rubber, such as epoxidized natural rubber (ENR), carbonyl telechelic natural rubber (CTNR) and hydroxyl telechelic natural rubber (HTNR). In principle, a PCL-based polyurethane is a biodegradable polyurethane, whereas a HTNR-based polyurethane is a bio-based polymer and does not easily degrade; although NR is a biopolymer, its biodegradation has not been widely studied, we found just one article reporting the biodegradation of NR/starch blend by bacteria isolated from soil.⁴⁴ Therefore, if a biodegradable segment, for

Table I. List of Chemicals

Chemical	Tradename/Producer	Specification
Natural rubber	Jana Concentrated Latex Co., Thailand	STR5 CV60 grade
Dibutyl tin dilaurate	Aldrich	Analytical grade (95%)
m-chloroperbenzoic acid	Fluka	Analytical grade (70%)
Poly(ϵ -caprolactone) diol ^a	Aldrich	Laboratory grade $\overline{M}_n = 530/2000$ g/mol T_m : 36–48°C, relative density at 25°C: 1.073 g/cm ³
Isophorone diisocyanate	Fluka	Analytical grade (98.0%)
Toluene-2,4-diisocyanate	Fluka	Analytical grade (90.0%)
Hexamethylene diisocyanate	Fluka	Analytical grade (98.0%)
Periodic acid	Himedia	Analytical grade (99.5%)
Sodium borohydride	Rankem	Analytical grade (98.0%)
Tetrahydrofuran	Fisher Scientific UK Limited	Analytical grade (99.8%)
1,4-Butanediol	Merck	Analytical grade (99.0%)

^aTwo grades: $\overline{M}_n = 530$ g/mol (liquid) and 2000 g/mol (wax).

instance PCL, were introduced into HTNR-based polyurethane, biodegradation should occur in the PCL segment and the HTNR segment could be recovered and reused.

Recently, a new bio-based polyurethane made from HTNR and PCL diol was reported by Panwiriyarat et al.⁴⁵ In this work polyurethane containing a high amount of isophorone diisocyanate was prepared and the effect of the HTNR amount on the mechanical properties of the resulting polymer was investigated. The NCO:OH molar ratio equaled to 2.85:1.00 and 1,4-butanediol (BDO) was used as chain extender. The formation of the urethane linkage and of allophanate groups was observed by FTIR analysis. The material resulted highly crosslinked and this was attributed to no phase separation between the hard and the soft segment. The hydrogen bonding between the PCL diol and the diisocyanate fragments was considered responsible of the high T_g observed. By addition of a small amount of HTNR in the formulation, the tensile properties, and tear strength of PU increased significantly. With a further increase of the HTNR content, the tensile behavior of PU was changed from a tough to a soft polymer.

Generally, the mechanical and thermal properties of polyurethane directly depend on the chemical composition, type and molecular weights of the soft and hard segments.^{3,4,46} Consequently in the present work we aimed at completing the previous study and we investigated the effect of the diisocyanate type and the molecular weights of the HTNR and the PCL diol on the mechanical and thermal properties of polyurethane containing a lower isocyanate content.

EXPERIMENTAL

Materials

Three types of diisocyanate were employed: isophorone diisocyanate (IPDI), toluene-2,4-diisocyanate (TDI) and hexamethylene

diisocyanate (HDI). Two commercial PCL diols were selected and their molecular weights were 530 and 2000 g/mol. HTNR was synthesized from solid NR and their molecular weights were 1700 and 2800 g/mol. All chemicals used are listed in Table I and their chemical structures are shown in Figure 1. The PCL diol was vacuum dried at 40°C for 24 h prior to use. Other chemicals were used as received.

Synthesis of Hydroxyl Telechelic Natural Rubber

Hydroxyl telechelic natural rubber (HTNR) was prepared by an oxidative chain cleavage reaction of natural rubber. The double bonds of NR were cleaved by using periodic acid at 30°C for 6 h in tetrahydrofuran to obtain a carbonyl telechelic natural rubber (CTNR). The carbonyl end-group in CTNR became hydroxyl end-group by using sodium borohydride. The reaction was carried out at 60°C for 6 h in tetrahydrofuran. All chemical structures were verified by ¹H-NMR spectroscopy and molar masses by gel permeation chromatography. Two number average

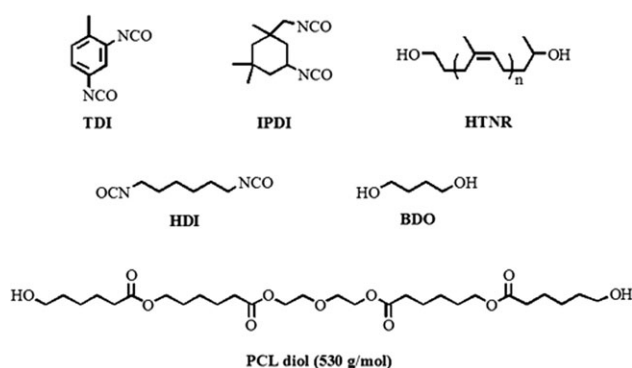


Figure 1. Chemical structure of HTNR, PCL diol, BDO, TDI, HDI, and IPDI.

Table II. Chemical Composition and Physical Properties of PU1-PU5

Code	Molar ratio				HS ^a (%)	Physical appearances ^b
	1.25 NCO	0.35 PCL	0.15 HTNR	0.5 BDO		
PU1	TDI	PCL ₅₃₀	HTNR ₁₇₀₀	✓	37.4	Y, S, ST
PU2	HDI	PCL ₅₃₀	HTNR ₁₇₀₀	✓	36.7	Y, H, O
PU3	IPDI	PCL ₅₃₀	HTNR ₁₇₀₀	✓	42.3	Y, S, ST
PU4	IPDI	PCL ₅₃₀	HTNR ₂₈₀₀	✓	34.8	Y, S, ST
PU5	IPDI	PCL ₂₀₀₀	HTNR ₁₇₀₀	✓	25.3	Y, S, O

^aHard segment (%) = 100 [weight of (isocyanate+chain extender)]/total weight.

^bY, yellowish; H, hard; S, soft; O, opaque; ST, semi-transparent.

molecular weights (M_n) of HTNR were prepared: 1700 and 2800 g/mol (referred to HTNR₁₇₀₀ and HTNR₂₈₀₀, respectively).

Synthesis of Polyurethane

Polyurethane (PU) was synthesized by a one-shot method. Three parameters were investigated: the molecular weight of the PCL diol (530 and 2000 g/mol), of HTNR (1700 and 2800 g/mol), and the diisocyanate structure. Three types of diisocyanate were employed (in this paper the abbreviation NCO will be used to indicate a diisocyanate molecule, not a single group): IPDI, TDI and HDI. The total diol content (OH) came from PCL diol, HTNR and 1,4-butanediol (BDO). Generally BDO acts as a chain extender and contains hydroxyl groups; therefore, BDO content was taken into account in the diol calculation of chemical components.⁴⁵ Chemical composition of the resulting PUs is listed in Table II. The molar ratio of NCO:OH was 1.25 : 1.00 while the molar ratio of PCL:HTNR:BDO was 0.35 : 0.15 : 0.50. A mixture of these diols was dissolved in THF (30 w/v%) and mixed with dibutyl tin dilaurate as a catalyst. A known amount of diisocyanate in THF was slowly added and the reaction temperature maintained at 60°C for 3 h. At the end of the reaction, the viscous polymer solution was poured into a glass mold and heated at 40°C for 3 h and at 60°C for 24 h to evaporate the solvent. The obtained square PU sheets were 15 cm x 15 cm with a thickness of 0.3–0.5 mm.

Testing of the Mechanical Properties

The die-cut specimens were prepared from the polyurethane sheets. The tensile properties (ASTM D 412C) and tear strength (ASTM D 624) were determined by a tensile testing machine (Lloyd®LR10K) at a crosshead speed of 500 mm/min. Eight specimens were tested for every sample. The average value and standard deviations were reported. The Young's modulus was determined from the initial slope of the linear portion of the stress–strain curves. The hardness shore A was carried out according to ASTM D2240 by a Shore Durometer® PTC 408.

Polymer Characterization

Thermogravimetric analysis (TGA) was carried out on a TA Instruments® TGA Q 100 with a heating rate of 10°C/min from room temperature to 600°C, under nitrogen atmosphere. TGA curves were recorded. The temperature at which a certain amount of weight loss occurred, e.g. 5, 10, and 50%, was determined from the TGA curves. A characteristic temperature (T_{peak}) that corresponds to the maximum rate of degradation

was determined from the derivative thermogravimetric curves (DTG).

Differential scanning calorimetry (DSC) was performed on a TA Instruments® DSC Q 100 under nitrogen atmosphere. In order to eliminate the effect of the thermal history, all samples were first heated from 20 to 200°C and then, were slowly cooled with a heating/cooling rate of 10°C/min and –10°C/min, respectively. Glass transition temperature (T_g) was recorded from the second heating scan in the range of –80 to 200°C.

The storage modulus (E'), the loss modulus (E'') and the loss tangent ($\tan \delta$) were measured by a Rheometric Scientific® DMTA V. The experiments were carried out in the dual-cantilever bending mode at a frequency of 1 Hz with a strain control of 0.01%, and the heating rate was 3°C/min. The temperature range was –80 to 200°C.

RESULTS AND DISCUSSION

The aim of this research study was to expand and complete the initial investigation of the synthesis of new bio-based and potentially biodegradable polyurethanes, based on polycaprolactone and natural rubber precursors. The attention was focused on the influence of the diisocyanate structure and on the diol molecular weight on the physical and thermal properties of the generated polyurethane sheets.

The molar ratio of precursors NCO:PCL:HTNR:BDO (NCO refers to a diisocyanate molecule, containing 2 isocyanate groups) to use in the formulations was selected from the preliminary study carried out. It was found that when the NCO:OH ratio was 0.75 : 1.00, film formation did not occur and a viscous liquid was obtained because of inadequate amounts of NCO groups.⁴⁵ The higher ratio (1.00 : 1.00) produced a very sticky film with no mechanical integrity. The desired films were finally generated when the NCO:OH ratio was 1.25 : 1.00.

The obtained PUs contained 25–42% of the hard segment (i.e., diisocyanate plus chain extender) as shown in Table II. The percentage of the hard segment depended also on the molecular weights of the starting materials. The physical appearances of PU by visual observation are described in Table II; the yellow color of PU derived from the presence of HTNR, while soft and semitransparent sheets were given by the samples containing

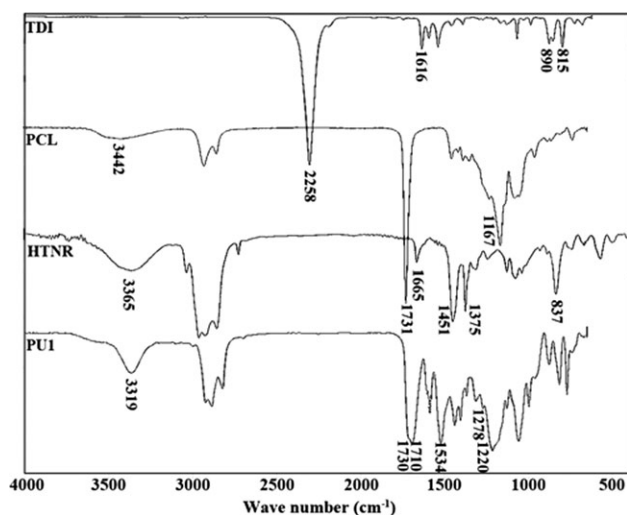


Figure 2. FTIR spectra of TDI, HTNR, PCL diol, and PU1.

TDI and IPDI. On the contrary PU2 prepared from HDI was hard and opaque.

The formation of a crosslinked network in PU due to the excess of isocyanate was investigated by performing solubility tests and FTIR analyses. No sample dissolved in chloroform and tetrahydrofuran which are the solvents used for the polymerization of PU.

Infrared spectra of the polyurethane films were carried out to check the formation of the urethane bonds: Figure 2 shows

Table III. FTIR Assignment of Precursors and Polyurethane

	Wavenumber	Assignment
PCL	3442 cm^{-1}	ν (O—H)
	1731 cm^{-1}	ν (C=O) of ester
	1167 cm^{-1}	ν (C—O) of ester
HTNR	3365 cm^{-1}	ν (O—H)
	2730–2900 cm^{-1}	ν (CH_2 , CH_3)
	1664 cm^{-1}	ν (C=C)
	1448, 1376 cm^{-1}	δ (CH_2 , CH_3)
TDI	834 cm^{-1}	δ (C=C—H)
	2258 cm^{-1}	ν (N=C=O)
	1721, 1781 cm^{-1}	Overtone of aromatic substitution
PU	1600–1500 cm^{-1}	ν (C=C) in aromatic compound
	815–890 cm^{-1}	δ (C=C—H)
	3319 cm^{-1}	ν (N—H), H-bonded
	1730 cm^{-1}	ν (C=O)
	1710 cm^{-1}	ν (C=O), H-bonded
	1534 cm^{-1}	δ (N—H) + ν (C—N)
	1310 cm^{-1}	δ (N—H) + ν (C—N)
	1220 cm^{-1}	Amide III + ν (C—O)

ν , stretching; δ , bending.

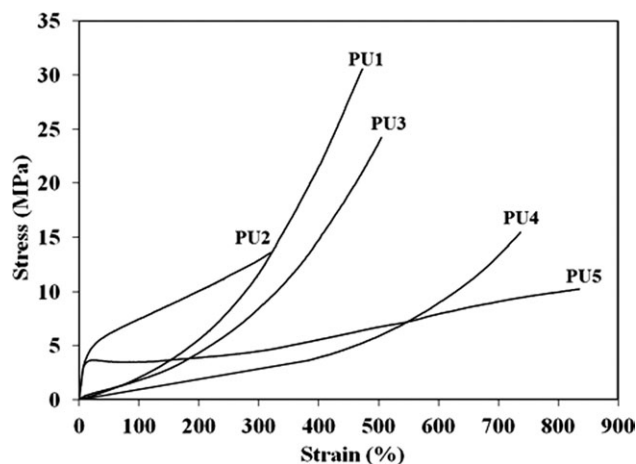


Figure 3. Stress-strain curves of PU1-PU5.

FTIR spectra of PCL diol, HTNR, TDI, and PU1 and in Table III the FTIR assignment of the precursors and PU are listed.^{47–49} The —OH absorption band of PCL diol and HTNR and the —N=C=O absorption band of diisocyanate were not observed in PU1, which showed new absorption bands in 4 regions: (1) at 1728 cm^{-1} , corresponding to the non-hydrogen bonded —C=O stretching; (2) at 1715 cm^{-1} , corresponding to the carbonyl stretching of the C=O hydrogen bonded with the NH group in the urethane linkage; (3) at 3360–3365 cm^{-1} , corresponding to the NH stretching vibration; (4) at 1525–1550 cm^{-1} , corresponding to the bending vibration. It was found that an excess of isocyanate generates allophanate groups and acylurea linkages that cause crosslinking in PU.^{2,50} The characteristic peaks of the allophanate group fall in 2 regions: (1) stretching vibrations at 1220, 1280, and 1310 cm^{-1} and (2) bending vibrations at 3298, 3267, and 3233 cm^{-1} .⁵¹ The present PUs showed the characteristic bands of the allophanate group at 1234, 1276 and 1304 cm^{-1} , and the absorption bands at 3233–3298 cm^{-1} were overlapped with the band of NH stretching at 3361 cm^{-1} . Generally, the excess of diisocyanate can react with water and generate an urea linkage before forming a biuret later. The wavenumbers of the signals of the biuret and the allophanate groups fall in the same region so it was believed that the allophanate was formed in our case because the samples were in a dry environment.

The effect of the diisocyanate (NCO) type was determined from the samples called PU1-PU3 and the effect of the molecular weight of PCL and HTNR was determined from samples PU3-PU5.

Effect of the Diisocyanate Type

On the Mechanical Properties. Three different molecular architectures of diisocyanate were employed: a linear aliphatic diisocyanate (HDI), an aromatic diisocyanate (TDI), and a cycloalkane diisocyanate (IPDI). The molecular weight of the PCL and HTNR used in this case was 530 g/mol and 1700 g/mol, respectively. Mechanical tests were carried out and the stress-strain curves of the polyurethanes (Figure 3) and their tensile properties (Table IV) have been obtained. It was observed that PU1 and PU3 showed rubber-like behavior with

Table IV. Effect of Various Type of Diisocyanate and Molecular Weight of Diol on the Mechanical Properties of PU1-PU5

Code	Tensile properties				Tear strength (N/mm)	Hardness (Shore A)
	E (MPa)	$E_{300\%}$ (MPa)	σ_b (MPa)	ϵ_b (%)		
PU1	1.9 ± 0.4	11.6 ± 1.0	28.4 ± 1.9	447 ± 52	32.0 ± 3.5	49 ± 3
PU2	37.1 ± 4.1	12.9 ± 1.1	15.0 ± 1.9	329 ± 21	57.7 ± 6.2	77 ± 3
PU3	2.2 ± 0.4	8.4 ± 1.0	24.3 ± 1.2	506 ± 10	38.3 ± 1.2	56 ± 1
PU4	0.9 ± 0.0	3.5 ± 0.5	15.6 ± 0.6	753 ± 14	29.9 ± 1.8	37 ± 2
PU5	49.0 ± 4.0	4.4 ± 0.6	10.0 ± 1.3	867 ± 44	45.0 ± 4.2	31 ± 2

no plastic yielding. An elastic deformation followed by yielding and a plastic deformation was observed in the PU2. The polyurethane derived from HDI (PU2) showed the highest Young's modulus (E) and the lowest elongation at break (ϵ_b). HDI is claimed to be a crystallizing diisocyanate² due to its linear structure; therefore, PU2 was expected to be a crystalline PU. Furthermore, its opacity should be the result of the crystallization of the hard segment. This assumption was verified by DSC analysis, as described later. The crystalline region of the hard segment acted as a physical crosslink providing a higher modulus and a lower elongation at break. The low tensile strength (σ_b) of PU2 was due to the relatively low ductility compared to PU1 and PU3. The effect of the crystallization of HDI was also responsible of the highest tear strength and hardness values (Table IV). Found for PU2.

According to Hepburn,¹ the effect of the methyl substituent in TDI and IPDI is dominant, and causes an asymmetrical structure leading to amorphous domains. This results in a large drop in the Young's modulus and tear strength and an increase in the flexibility. This phenomenon has been also observed in the present study. The tensile behavior of PU1 and PU3 looked like a typical rubber: very low Young's modulus, high tensile strength, and high elongation at break. Their hardness and tear strength were ranked in the following order: PU1 < PU3 < PU2 (Table IV). We could observe that the molecular structure of the diisocyanate played a major role on the mechanical properties of PU. The linear diisocyanate showed a remarkable difference in the tensile behavior and the mechanical properties from the cyclic one, but TDI and IPDI did not show significant difference in those properties, except that the elongation at break of PU3 was higher than that of PU1. The modulus at 300% ($E_{300\%}$), an important property of elastomers, is the stress at a 300% strain. All PUs showed a high $E_{300\%}$, i.e., in the range of 8–13 MPa, indicating a strong elastomer. Furukawa et al.⁵² reported the structure-properties relationship of caprolactone-based PU with 2 types of diisocyanates: 1,2-bis(isocyanate)ethoxyethane (TEGDI) and HDI. The polyurethane elastomer was prepared by using a two-shots method and the ratio of NCO:OH was 1.05 : 1.00. They found that the Young's modulus was in the range of 0.8–15 MPa, which was lower than that of the present study, and the tensile strength was 1.0–42 MPa, which was a larger range than this study. The elongation at break of those PUs was in the same range as found in this study, while the TEGDI-based PU showed a larger strain at break and lower Young's modulus than the HDI ones.

On the Thermal Properties. The thermal behavior of the polyurethanes was investigated by DSC and TGA. The DSC thermograms of the soft segments (the diol precursors) and the hard segment (the diisocyanate plus chain extender) recorded from the second heating scan are illustrated in Figure 4(a,b), respectively. The hard segment model was obtained from the polyurethane sheet containing only diisocyanate and the chain extender (BDO), in the molar ratio of 1.25 : 1.00. PCL diols had a double melting peak (T_m): at $-9/15^\circ\text{C}$ for the low molecular weight (PCL₅₃₀) and $44/49^\circ\text{C}$ for the high molecular weight (PCL₂₀₀₀), similar to the observations by Kim et al.¹⁷ There was an unclear transition temperature at -78°C in the PCL₅₃₀ sample [Figure 4(a)]. This transition occurred at the beginning of the investigation, and it could be due to a shift of the base line. Unfortunately, the T_g of PCL₅₃₀ was not detectable from the cooling scan. The crystallization temperature (T_c) obtained from a cooling scan was noticeable in PCL diols (data not shown here). The HTNRs were amorphous and their T_g values were in the same range, -60°C to -58°C . The differences in molecular weight between both HTNRs were not so high as that of the PCL diols, and this led to a similar T_g . The crystallization behavior of the hard segment strongly depended on diisocyanate structure as showed in Figure 4(b). A melting peak was observed in HDI-based hard segment: it displayed relatively low T_g at 28°C and T_m at 175°C , whereas the IPDI-based and TDI-based hard segment showed only T_g in the same range: at 109°C and 107°C , respectively.

The DSC results of samples PU1-PU3 are shown in Figure 4(c). PU1 and PU3 were amorphous whereas PU2 was a semicrystalline polymer because of the crystallinity of the HDI hard segment. PU2 showed T_m at 126°C [Figure 4(c)] and T_c obtained from a cooling scan, at 63°C . The presence of the endothermic peak in PU at $\sim 130^\circ\text{C}$ due to HDI is reported by Furukawa et al.⁵² Although the PCL diol was a crystallizable material, it could not be crystallized in the present PUs. This phenomenon was verified by PU5 containing PCL₂₀₀₀ in which no melting peak was observed. As a result, the crystalline PU (PU2) had a different tensile behavior from the amorphous PU (PU1 and PU3) and, at the same time, it had the highest Young's modulus.

PU1-PU3 had double T_g ; in particular, T_g s of PU1 and PU3 were similar, -55°C and 25°C . Although the T_g s of the TDI and IPDI hard segment were high, 107°C and 109°C , respectively, they did not appear in PU1 and PU3. Undoubtedly, the

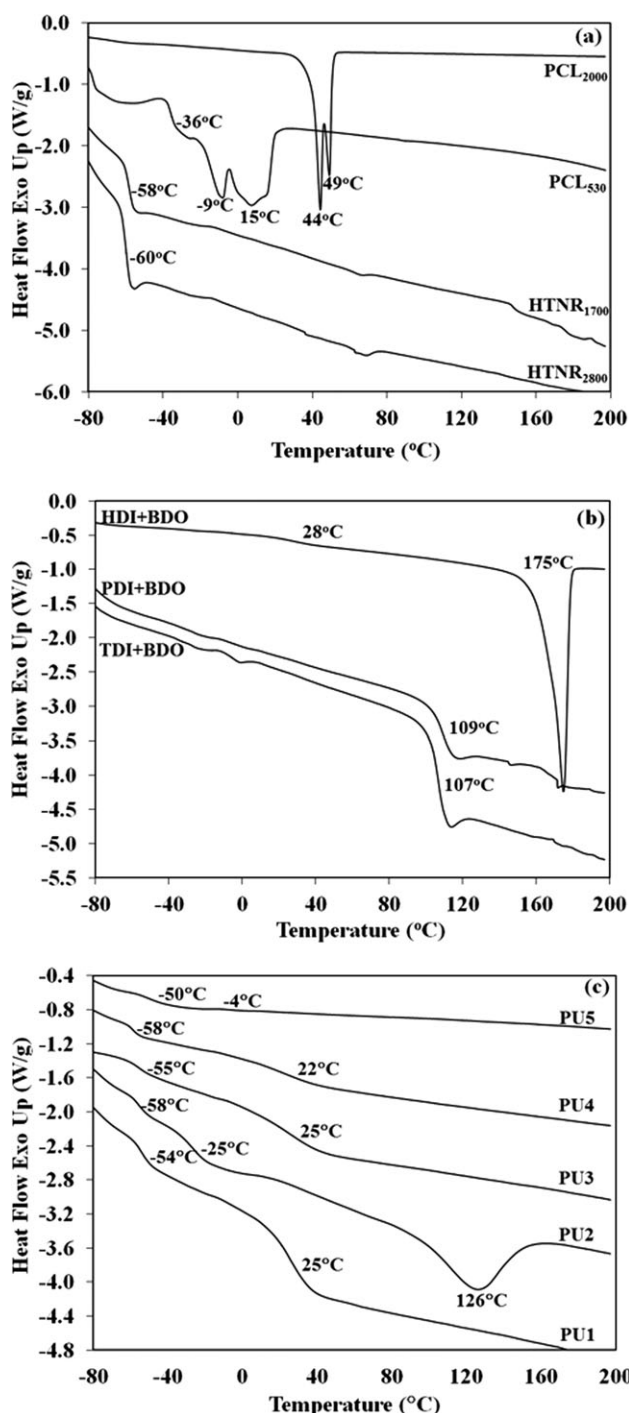


Figure 4. DSC thermograms recorded from the 2nd heating scan: (a) diol precursors; (b) hard segments (NCO+BDO); and (c) PU1-PU5.

T_g at -55°C was due to the HTNR segment. It was believed that the T_g at 25°C belonged to the PCL diol segment that had hydrogen bonds with the hard segment. Only the PCL diol, but not the HTNR, in the polyurethane is able to form hydrogen bonding with the hard segment.⁴⁵ Therefore, this T_g (25°C) was higher than the T_g of the virgin PCL₅₃₀ and lower than the T_g of the TDI and IPDI. The analysis of PU2 showed that it had two T_g s at -58°C and -25°C ; the lower T_g was assigned to the

HTNR segment and the higher one to the PCL diol, hydrogen bonded with the HDI hard segment. We can assume that the lowest T_g in PU2 is due to the segmental hexamethylene contribution.² No phase separation between the PCL diol and the IPDI hard segment in the polyurethane was observed,⁴⁵ consequently, a phase separation between the hard segment and the soft segment in the present PUs was not found.

The transition temperatures of the PUs were also determined by using dynamic mechanical thermal analysis (DMTA). Figure 5 shows the dynamic mechanical curve of PU1-PU3 including the storage modulus, the loss modulus and the loss tangent as a function of temperature. The molecular architecture of the diisocyanate also played a major role in the dynamic mechanical thermal properties. The more flexible, linear structure of the HDI was responsible of a low storage modulus and a low α transition temperature of PU2. The rise in E' of PU2 may be due to its crystallinity or its sensitivity in microphase separation. Furukawa et al.⁵² reported that the rise in E' of PCL-based PU is due to the recrystallization of the soft segment. According to Samy et al.,⁵³ the rise in E' of polyurethane relates to the microphase separation. TDI (PU1) and IPDI (PU3) provided similar DMTA curves. The loss modulus shown in Figure 5(b) was also strongly dependent on the molecular structure of the diisocyanate. The flexible structure of HDI in PU2 caused a sudden drop in E'' at approximately -23°C , whereas the rigidity of TDI and IPDI contributed to the higher E'' at this temperature. Figure 5(c) represents the $\tan \delta$ of PU1-PU5. As found from the DSC results, PU1-PU3 showed multiple transition temperatures with no significant differences between PU1 and PU3. PU1 and PU3 showed α transition temperature at 49°C , which arose from the relaxation of the PCL diol that hydrogen bonded with the diisocyanate. The α transition temperature of the TDI and IPDI hard segment was 56 and 70°C , respectively. A subglass transition temperature (β relaxation) of PU1 and PU3 was detected at -50°C , and it derived from the HTNR segment. PU2 instead exhibited 3 transition temperatures: 65 , -15 , and -76°C ; it was assumed the α and β transition temperatures were at -15°C and -76°C , respectively, while the relaxation temperature at 65°C ($>T_g$) might be associated with the crystallinity.

Thermo gravimetric analysis of the samples was carried out. The thermal stability of the diol precursors (PCL diols, HTNRs, and BDO), the hard segments (diisocyanate+BDO) and PUs are illustrated in Figure 6 (A weight loss at a certain temperature from the TGA thermogram is also listed in Table V). A T_{peak} in Table V was the temperature at which a rapid drop in weight loss took place. The thermal stability of the diols depended on their chemical structure and molecular weight [Figure 6(a)]. The lowest thermal degradation temperature appeared in the BDO due to its lowest molecular weight. PCL₂₀₀₀ showed higher thermal stability than PCL₅₃₀, whereas both HTNRs had similar thermal degradation temperatures. Figure 6(b) illustrates TGA curves of the hard segment (diisocyanate and BDO): a slight difference in the thermal stability between the TDI and the IPDI hard segment was observed, therefore there was an insignificant difference in the thermal stability between PU1 and PU3 [Figure 6(c)]. The HDI hard segment had a higher thermal

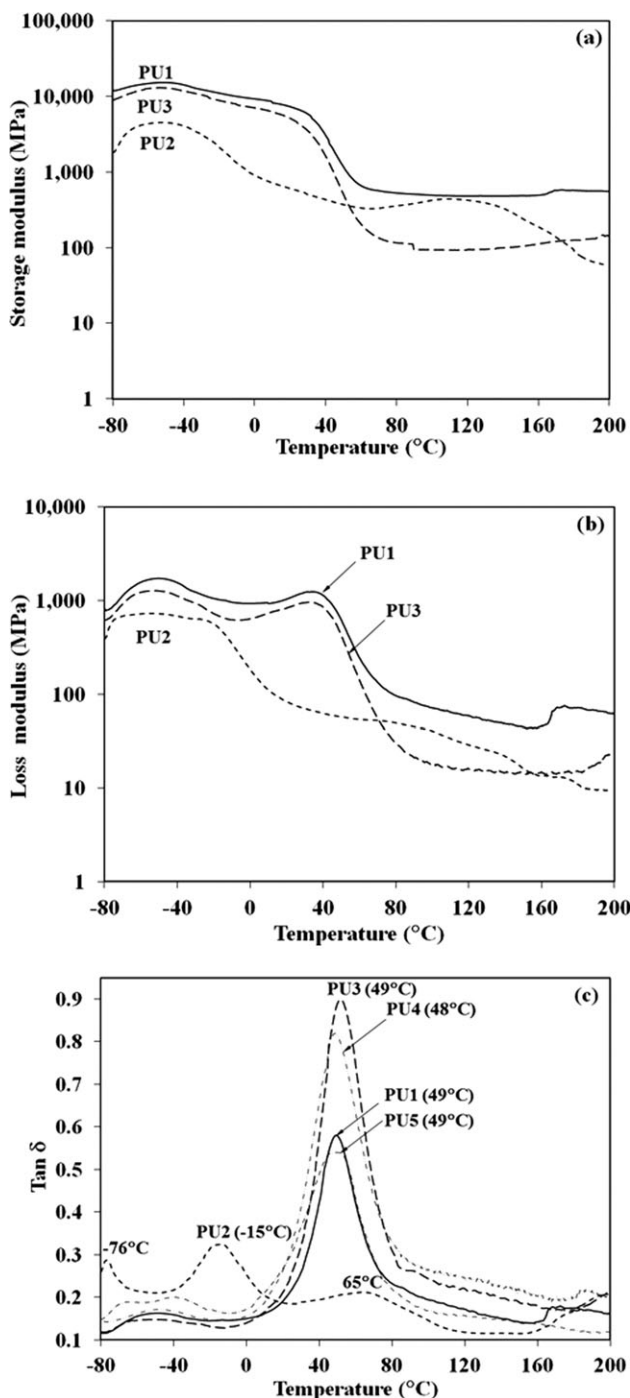


Figure 5. Dynamic mechanical curves as a function of temperature: (a) the storage modulus of PU1-PU3, (b) the loss modulus of PU1-PU3, and (c) the $\tan \delta$ of PU1-PU5.

stability than the TDI and IPDI, even though the HDI has a linear molecular structure and can form crystalline domains. As a result, PU2 had the highest thermal stability. These results reasonably agree with those from the study of Wei et al.⁵⁴

Effect of the Molecular Weight of the Diols

On the Mechanical Properties. The use of polyols with different molecular weights allowed an investigation of the effect of

the polyol chain length. The synthesized polymers had different hard segment contents that depended on the polyol molecular weight: 42.3, 34.8, and 25.3% for PCL₅₃₀-HTNR₁₇₀₀ (PU3), PCL₅₃₀-HTNR₂₈₀₀ (PU4) and PCL₂₀₀₀-HTNR₁₇₀₀ (PU5), respectively. The physical appearance of the films is described in Table II. PU5 was opaque although it consisted of IPDI, the noncrystallizing diisocyanate. We hypothesized that the opacity was not due to crystallization as occurred in PU2, but it might arise

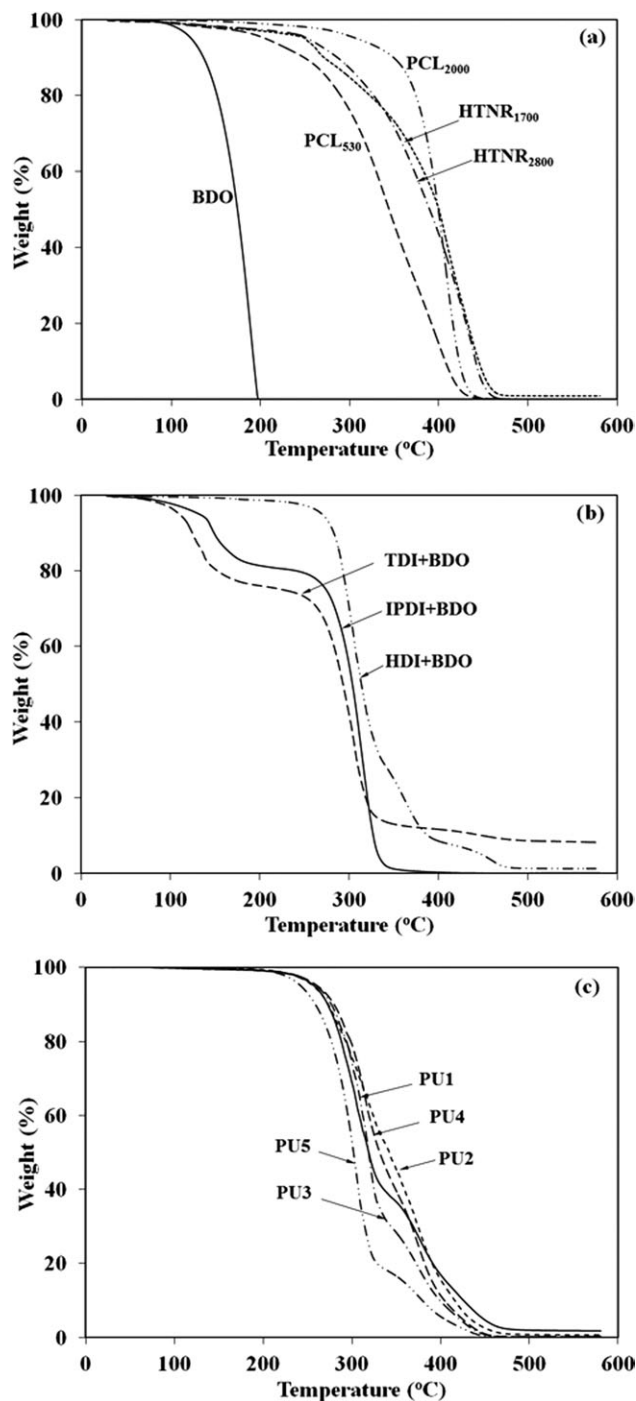


Figure 6. TGA thermograms as a function of temperature: (a) diol precursors, (b) hard segments (NCO+BDO), and (c) PU1-PU5.

Table V. TGA Data of the Precursors, Hard Segment (NCO+BDO) and PU1-PU5

Materials	T_5^a (°C)	T_{10}^a (°C)	T_{50}^a (°C)	T_{90}^a (°C)	T_{peak}^b (°C)
BDO	123	136	174	192	189
PCL ₅₃₀	206	249	344	407	339, 398
PCL ₂₀₀₀	308	350	399	422	407
HTNR ₁₇₀₀	250	272	400	445	263, 407
HTNR ₂₈₀₀	253	287	390	441	439
TDI+BDO	110	124	293	450	124, 306, 452
HDI+BDO	270	283	314	388	304, 365, 460
IPDI+BDO	132	149	304	327	146, 314
PU1	257	272	318	425	304, 378
PU2	256	273	342	415	305, 374
PU3	260	276	318	399	320, 377
PU4	261	279	331	404	315, 375
PU5	242	259	301	379	304, 378

^aData obtained from the TGA curve.

^bData obtained from the DTG curve.

from the high phase segregation because by the high molecular weight of PCL₂₀₀₀: when the DSC thermogram [Figure 4(c)] was examined, no T_m was detected and this confirmed the assumption.

The influence of the molecular weight on the stress–strain curves is illustrated in Figure 3. PU3 and PU4 exhibited a typical rubbery characteristic with a high elongation at break and a low modulus. PU5 initially underwent an elastic deformation followed by a yielding and a plastic deformation. The molecular weight of the PCL diol influenced the tensile behavior of PU more than that of the HTNR. The effect of the molecular weight of the diols on the tensile properties, tear strength and hardness is listed in Table IV. By increasing the molecular weight of the PCL diol (PU3 vs. PU5), the Young's modulus and the elongation at break increased but the tensile strength decreased. It may be assumed that the crystallinity of the PCL₂₀₀₀ give a major contribution to the higher modulus in PU5. In addition, there would be a higher tensile strength and lower elongation at break if the crystallinity of PCL₂₀₀₀ was dominant. However, PU5 had an amorphous nature as determined by the DSC characterization. This inconsistency could be explained in terms of the content of the hard segment that was associated with the crosslink density. The hard segment content was calculated based on the weight of the chemicals. By using a constant molar ratio, the concentration of chemicals changed owing to their different molecular weight, thus, PU3 had a greater hard segment content than PU5. If the higher molecular weight of the PCL diol exerted a major influence on the Young's modulus, the hard segment content may exert a major influence on the tensile strength and elongation at break. The higher molecular weight of the PCL diol increased the tear strength, which agreed with the increase in the Young's modulus. Concerning PU5, a decrease in the hardness may be due to the higher flexibility of the longer chain of the soft segment (PCL₂₀₀₀) and the low hard segment content: in fact it was noticed that PU5 had the lowest hard segment content among the PU1-PU5 samples,

and this led it to have the lowest hardness and the highest elongation at break.

The higher molecular weight of HTNR decreased the mechanical properties, except for the elongation at break, as seen comparing PU3 and PU4. These differences may result from an increase in the chain flexibility and a decrease in the hard segment content due to the longer chain length of the HTNR.

On the Thermal Properties. The influence of the molecular weight of the diols on the thermal properties is shown in Figure 4(c). PU3-PU5 showed amorphous characteristics, which is not surprising as crystallization of the soft segment rarely occurs at molecular weights inferior to 2000 g/mol.¹ Considering the molecular weight of the PCL diol used, PU3 and PU5 showed 2 T_g s (the low- T_g and the high- T_g): -55°C and 25°C in PU3 and -50°C and -4°C in PU5. It appeared that the higher molecular weight of the PCL diol was responsible of the lower T_g , e.g., from 25°C in PU3 to be -4°C in PU5. The effect of the molecular weight of the PCL diol on the T_g may be related to the hard segment content: a lower crosslink density, due to a lower hard segment content, could have produced a lower T_g in PU5 than in PU3. This phenomenon could be explained by the fact that when chain length between the crosslinks increases, a higher flexibility of the material is obtained. This same observation was also clearly found in the cooling scan (data not shown here). The HTNR chain length induced a little change in T_g , with PU3 having slightly higher T_g s than PU4, therefore, in conclusion, it was observed that the molecular weight of the PCL diol had more influence on the T_g value than that of the HTNR.

In contrast to the DSC results, the α transition temperatures derived from the DMTA of the PU3-PU5 were in the same range (49°C), and their DMTA curves were similar [Figure 6(c)]. The thermal stability of PU4 seemed to be the lowest (Table V) but generally the thermal degradation temperatures of PU3-PU5 were in the same range.

CONCLUSIONS

The aim of this research work was to synthesize novel bio-based and potentially biodegradable polyurethanes. Different formulations were conceived and conditions were optimized in order to obtain thin, flexible films. A study of the influence of selected parameters on the mechanical and thermal properties of the resulting materials was carried out. It was found that the molecular architecture of diisocyanate and molecular weight of diol played an important role on the mechanical properties and materials characteristics. The linear structure of hexamethylene diisocyanate (HDI) was able to crystallize leading to a crystalline PU (PU2), whereas the asymmetrical cyclic structure of toluene-2,4-diisocyanate (TDI), and isophorone diisocyanate (IPDI) produced amorphous PU (PU1 and PU3). This morphology affected the tensile behavior and the mechanical properties. The crystalline region acted as physical crosslink enhancing the Young's modulus and reducing the elongation at break, and it was responsible of the plastic yielding during tensile testing. In contrast, the amorphous characteristic of PU1 and PU3 was the cause of the rubber-like behavior, i.e., very low Young's modulus and high elongation at break. The crystallinity also increased the tear strength, the hardness and the thermal stability of PU. There was no significant difference between TDI and IPDI on the mechanical properties and the materials characteristics. Although PCL diols could crystallize, they could not provide crystallization in the generated PU. The increase in the molecular weight of PCL diol changed tensile performance of PU from the rubber-like to the plastic-like behavior. Another factor that controlled the mechanical properties and features of PU was the hard segment content, which was related to the crosslink density. No phase separation between the hard and the soft segment was observed because of the hydrogen bonding formed between PCL diol and diisocyanate; T_g values determined from DSC and DMTA substantiated this assumption.

ACKNOWLEDGMENTS

The authors acknowledge financial support from the National Research Council of Thailand (NRCT) and the French-Thai Cooperation Program in Higher Education and Research.

REFERENCES

- Hepburn, C. *Polyurethane Elastomers*, 2nd ed; Elsevier Science Publishers: New York, **1992**; p 1.
- Prisacariu, C. *Polyurethane Elastomers from Morphology to Mechanical Aspects*; Spinger Wien New York: New York, **2011**.
- Li, F.; Hou, J.; Zhu, W.; Zhang, X.; Xu, M.; Luo, X.; Ma, D.; Kim, B. K. *J. Appl. Polym. Sci.* **1996**, *62*, 631.
- Lan, P. N.; Corneillie, S.; Schacht, E.; Davies, M.; Shard, A. *Biomaterials* **1996**, *17*, 2273.
- Wang, W.; Ping, P.; Yu, H.; Chen, X.; Jing, X. *J. Polym. Sci. A Polym. Chem.* **2006**, *44*, 5505.
- Ping, P.; Wang, W.; Chen, X.; Jing, X. *J. Polym. Sci. B Polym. Phys.* **2007**, *45*, 557.
- Skarja, G. A.; Woodhouse, K. A. *J. Appl. Polym. Sci.* **2000**, *75*, 1522.
- Chiou, B. S.; Schoen, P. E. *J. Appl. Polym. Sci.* **2002**, *83*, 212.
- Rogulska, M.; Kultys, A.; Pikus, S. *J. Appl. Polym. Sci.* **2008**, *110*, 1677.
- D'Arlas, B. F.; Rueda, L.; Caba, K.; Mondragon, I.; Eceiza, A. *Polym. Eng. Sci.* **2008**, *48*, 519.
- Maafi, E. M.; Malek, F.; Tighzert, L. *J. Appl. Polym. Sci.* **2010**, *115*, 3651.
- Gorna, K.; Gogolewski, S. *Polym. Degrad. Stab.* **2002**, *75*, 113.
- Gorna, K.; Polowinski, S.; Gogolewski, S. *J. Polym. Sci. A Polym. Chem.* **2002**, *40*, 156.
- Sarkar, D.; Yang, J. C.; Gupta, A. S.; Lopina, S. T. *J. Biomed. Mater. Res A.* **2009**, *90*, 263.
- Watnabe, A.; Takebayashi, Y.; Ohtsubo, T.; Furukawa, M. *J. Appl. Polym. Sci.* **2009**, *114*, 246.
- Gong, C. Y.; Fu, S. Z.; Gu, Y. C.; Liu, C. B.; Kan, B.; Deng, H. X.; Luo, F.; Qian, Z. Y. *J. Appl. Polym. Sci.* **2009**, *113*, 1111.
- Kim, B. K.; Lee, S. Y.; Xu, M. *Polymer* **1996**, *37*, 5781.
- Bogdanov, B.; Toncheva, V.; Schacht, E.; Finelli, L.; Sarti, B.; Scandola, M. *Polymer* **1999**, *40*, 3171.
- Bakare, I. O.; Pavithran, C.; Okieimen, F. E.; Pillai, C. K. *J. Appl. Polym. Sci.* **2008**, *109*, 3292.
- Tu, Y. C.; Suppes, G. J.; Hsieh, F. H. *J. Appl. Polym. Sci.* **2009**, *111*, 1311.
- Chian, K. S.; Gan, L. H. *J. Appl. Polym. Sci.* **1998**, *68*, 509.
- Jalilian, M.; Yeganeh, H.; Haghighi, M. N. *Polym. Int.* **2008**, *57*, 1385.
- Lligadas, G.; Ronda, J. C.; Galia, M.; Biermann, U.; Metzger, J. O. *J. Polym. Sci. A Polym. Chem.* **2006**, *44*, 634.
- Begines, B.; Zamora, F.; Roffe, I.; Mancera, Galbis, J. A. *J. Polym. Sci. A Polym. Chem.* **2011**, *49*, 1953.
- Barikani, M.; Honarkar, H.; Barikani, M. *J. Appl. Polym. Sci.* **2009**, *112*, 3157.
- Paul, C. J.; Gopinathan Nair, M. R. *Polym. Eng. Sci.* **1998**, *38*, 440.
- Cherian, A. B.; Thachil, E. T. *J. Appl. Polym. Sci.* **2004**, *94*, 1956.
- Sun, X.; Ni, X. *J. Appl. Polym. Sci.* **2004**, *94*, 2286.
- Gopakumar, S.; Paul, C. J.; Nair, M. R. G. *Mater. Sci-Poland.* **2005**, *23*, 227.
- Cherian, A. B.; Abraham, B. T.; Thachil, E. T. *J. Appl. Polym. Sci.* **2006**, *100*, 449.
- Kébir, N.; Campistrion, I.; Laguerre, A.; Pilard, J. F.; Bunel, C.; Couvercelle, J. P. *E-Polymers* **2006**, *48*, 1.
- Kébir, N.; Campistrion, I.; Laguerre, A.; Pilard, J. F.; Bunel, C.; Jouenne, T. *Biomaterials* **2007**, *28*, 4200.
- Radhakrishnan Nair, M. N.; Gopinathan Nair, M. R. *J. Mater. Sci.* **2008**, *43*, 738.

34. Chandrasekharan Nair, R.; Gopakumar, S.; Gopinathan Nair, M. R. *J. Appl. Polym. Sci.* **2007**, *103*, 955.
35. Sukumar, P.; Jayashree, V.; Gopinathan Nair, M. R.; Radhakrishnan Nair, M. N. *J. Appl. Polym. Sci.* **2009**, *111*, 19.
36. Radhakrishnan Nair, M. N.; Sukumar, P.; Jayashree, V.; Gopinathan Nair, M. R. *Polym. Bull.* **2010**, *65*, 83.
37. Saetung, A.; Rungvichaniwat, A.; Campistron, I.; Klinpituksa, P.; Laguerre, A.; Phinyocheep, P.; Doutres, O.; Pilard, J. F. *J. Appl. Polym. Sci.* **2010**, *117*, 828.
38. Saetung, A.; Rungvichaniwat, A.; Campistron, I.; Klinpituksa, P.; Laguerre, A.; Phinyocheep, P.; Doutres, O.; Pilard, J. F. *J. Appl. Polym. Sci.* **2010**, *117*, 1279.
39. Kébir, N.; Campistron, I.; Laguerre, A.; Pilard, J. F.; Bunel, C. *J. Appl. Polym. Sci.* **2011**, *122*, 1677.
40. Matsui, M.; Munaro, M.; Akcelrud, L. C. *J. Polym. Res.* **2011**, *18*, 2255.
41. Zia, K. M.; Zuber, M.; Barikani, M.; Bhatti I. A.; Khan, M. B. *Coll. Surf B Biointer.* **2009**, *72*, 248.
42. Wang, Y.; Xu, W.; Chen, Y. *Coll. Surf B Biointer* **2010**, *81*, 629.
43. Wan, M.; Baek, D. K.; Cho, J. H.; Kang, I. K. *J. Mater. Sci.: Mater. Med.*, **2004**, *15*, 1079.
44. Watcharakul, S.; Umsakul, K.; Hodgson, B.; Chumeka, W.; Tanrattanakul, V. *Electro. J. Biotechnol.* **2011**, *15*, DOI: 10.2225.
45. Panwiriyarat, W.; Tanrattanakul, V.; Pilard, J. F.; Pasetto, P.; Khaokong, C. *Adv. Sci. Lett.* **2013**, *19*, 1016.
46. Mondal, S.; Hu, J. L. *Polym. Int.* **2006**, *55*, 1013.
47. Khan, A. S.; Ahmed, Z.; Edirisinghe, M. J.; Wong, F. S. L.; Rehman, I. U. *Acta. Biomaterialia.* **2008**, *4*, 1275.
48. Romanova, V.; Begishev, V.; Karmanov, V.; Kondyurin, A.; Maitz, M. F. *J. Raman. Spectrosc.* **2002**, *33*, 769.
49. Hercule, K. M.; Yan, Z.; Christophe, M. M. *Int. J. Chem.* **2011**, *3*, 88.
50. Hepburn, C. *Polyurethane Elastomer*, 2nd ed; Elsevier Applied Science LT: New York, **1991**.
51. Thomas, V.; Muthu, J. *J. Mater. Sci.: Mater. Med.* **2008**, *19*, 2721.
52. Furukawa, M.; Mitsui, Y.; Fukumaru, T.; Kojio, K. *Polymer* **2005**, 10817.
53. Samy, A. M.; Joshua U. O. *Prog. Polym. Sci.* **2009**, *34*, 1283.
54. Wei, Y.; Cheng, F.; Li, H.; Yu, J. *J. Sci. Ind. Res.* **2005**, *64*, 435.